Available at www.sciencedirect.com
ScienceDirect
journal homepage: www.elsevier.com/locate/bbe

Original Research Article

Measurements comparison of finger joint angles in hand postures between an sEMG armband and a sensory glove

Antonio Pallotti [a], *Giancarlo Orengo* [b,*], *Giovanni Saggio* [b]

[a] *Department of Management and Law, University of Rome Tor Vergata, Via Columbia 2, 00133 Roma, Italy*
[b] *Department of Electronics Engineering, University of Rome Tor Vergata, via Politecnico 1, 00133 Roma, Italy*

ARTICLE INFO

Article history:
Received 16 April 2020
Received in revised form
15 January 2021
Accepted 9 March 2021
Available online 7 May 2021

Keywords:
Wearable device
Myoelectric armband
Surface electromyography
Finger angle measurement

ABSTRACT

This study compares the simultaneous measurements of finger joint angles obtained with a myoelectric armband (Myo), composed of eight surface electromyography (sEMG) sensors mounted on an elastic support, and a data glove, equipped with ten flex sensor on metacarpal and proximal finger joints.

The flexion angles of all finger joints in four hand postures, that is open hand, closed hand and grasping two 3D printed molds of different size, were measured with a manual goniometer, and used to create, for each finger joint, a linear model from the measurement of the corresponding flex sensor in an electronic glove, as well as a regression model from the simultaneous measurements of 8 sEMG sensors of the Myo armband. The regression models were extracted testing different algorithms from the Matlab Regression Learner Toolbox. The performance of the models of the two wearable devices were evaluated and compared, applying a standard test, taken from literature on sensory gloves to evaluate the repeatability, reproducibility and reliability of finger joint measurements. These results were also compared with those reported by published works that followed the same standard test, using data gloves based on different sensing technologies. This work aims to demonstrate that the sEMG armbands can be applied to register the static postures of each finger joint with almost the same accuracy of sensory gloves.

1. Introduction

Standing the high degree of freedom of the human hand, the primary challenge is how to transfer its capabilities not only for multifingered object manipulation [1], but also for evaluation of health status and support for diagnosis in neurological and motor diseases [2]. It underlies advanced artificial intelligence robotics and its related disciplines and applications.

* Corresponding author.
E-mail address: orengo@uniroma2.it (G. Orengo).
https://doi.org/10.1016/j.bbe.2021.03.003

Robotic hand control systems are coded to handle specific objects with their corresponding robotic hands. While humans can easily solve their hand manipulation tasks using skills and experiences [1], object manipulation algorithms of robotic hand control systems must have human-like manipulation and real-time operation capabilities, even if the degree of freedom (DoF) of robotic hands is often less than the 27 DoFs of a human hand. To this aim, sensory gloves have been widespread in recent years, equipped with resistive flex sensors and/or inertial sensor to recognize hand gestures [3], and in particular to apply to deaf-mute people to discriminate the Italian Sign Language [4], or the American Sign Language with capacitive strain sensors to add hand proprioception and tactile sensing [5], as well as a sequence of hand gestures [6], or to measure the finger joint angles [7]. More advanced electronic gloves, also equipped with tactile sensors, allow realistic human hand-like features for prosthetic hands of hand amputees [8], haptic feedback for remote object sensing [9,10], or for gestural control in medical telepresence [11]. However, the sensory gloves have often some disadvantages such as: a) they are not comfortable to wear for a long time, b) if completely closed, they do not make the skin breathe and reduce the tactile sensitivity, c) the same device cannot fit hands of different sizes, although many researches on textile sensors, which may be breathable and elastic, has made these shortcomings no longer a big issue. Nevertheless, different curvature in the finger joints between the small and big hands can affect the angle measurement. On the other hand, data gloves based on inertial sensor are not easy to wear and they need both sophisticated algorithms to perform long-time measurements and integration of information coming also from magnetic sensors [12]. A last drawback is that data gloves need to connect to an electronic board for real-time data acquisition, equipped with a radiofrequency transmitter to a local or remote processing unit, for monitoring operations, or a memory to store data, for periodic monitoring operations. The problem of data transmission may occur in data loss, energy expenditure and sniffing by third parties.

On the other hand, surface electromyography (sEMG) is a noninvasive technique, which can allow the control of the prosthetic hand through the muscle activating signals of the forearm. In fact, the developed models allow the estimation of fingers' patterns in hand amputees [13,14]. Obtaining the sEMG signals from single surface electrodes has advantages in selecting muscles that move the hand, but the sEMG electrodes must be positioned with great accuracy over the corresponding muscle. Moreover, the sEMG signals corresponding to finger muscle activation are generally smaller in amplitude and more affected by noise than those of hand movement, because they undergo nonlinear attenuation and filtering by forearm tissues, lying in deeper layers of the forearm than those related to the hand movement. Therefore, several electrodes are generally used to provide the information required to disambiguate finger movements [13].

On the other hand, off the shelf and scientifically validated armbands based on sEMG sensors caught our interest, because, on the one side, they integrate everything is required to transfer data to a smartphone or a laptop, on the other side, they are easily worn and fit to arms of different sizes, minimizing the number of possible errors. For example, a flexible surface electrode band integrating 32 contacts was used in [15] to disambiguate 12 hand/wrist gestures.

The sEMG armbands, like the Myo of the Thalmic Labs or gForce200/Pro of OYMotion, which integrate 8 sEMG electrodes equally spaced around an elastic armband to cover all the forearm muscles, only need to keep the same orientation around the arm, to provide enough information to disambiguate the selected movements. As a result, applications based on sEMG armbands are more compact and look better, even if the potential of such devices is not yet fully exploited, for example in the application in work environments, where they could monitor the muscle fatigue of the workers, as successfully attempted in [16], where an elastic bracelet with 6 sEMG equally spaced electrodes was applied to disambiguate 6 hand/wrist gestures and 3 force levels.

Although each sEMG electrode usually cover more than one muscle, as will be shown below, the Myo armband has been successfully applied to classify predetermined patterns for hand gesture recognition [17,18], or human-robot interface [19], reaching similar performances to data gloves equipped with integration of flex and inertial (IMU) sensors [4].

In robotic and prosthetic hands, however, control strategies based on simultaneous and proportional control (SPC) of finger movements are preferred over those which can estimate only hand patterns. To this aim, multichannel sEMG signals were already applied to continuously decode finger joint angles. Ngeo had already proposed in 2014 to estimate the SPC of multiple DOFs [20]. Chen proposed to identify motor unit discharges during natural movements with sEMG electrode grids and to correlate them with finger angles [21]. In both projects, however, the number of channels involved may be too many for practical applications. Hioki tried to estimate multiple finger angles with only four sEMG sensors, although placed only on the flexor muscles, training a recurrent neural network (RNN), that used a feedback stream and time delay factors integrated into the perceptron system [22]. The Myo armband, covering the all sides of the arm with 8 sEMG electrodes, is able to monitor also the extensor muscles, which are actives when the hand is opening. Other authors demonstrated SPC estimation of finger movements after recognizing hand postures or gestures: for example, Pan proposed a setup similar to ours, but with 8 discrete sensors (Trigno), to continuously decode finger joint angles after a classifier recognized which static wrist motion the subject was conducting [23], Wang, using a public dataset [24,25], recently attempted to classify first 6 grasping hand movements, then to decode 20 joint angles of each gesture with a long-short term recurrent memory network, generally used to model temporal sequences [26]. However, these two last methods limit their operability to hand gesture recognition.

The sEMG armbands were never used for SPC estimation of finger joint angles. First of all, the followed procedure for sEMG data collection with an armband obviates the need for accurate placement of single sEMG sensors, because the sEMG armbands operate with dry sensors that do not require skin cleaning, but only to be worn with the 4th sensor in the sagittal plane of the forearm to avoid displacement errors [27], thus providing an easy, non-invasive and safe tool for sEMG signal acquisition and analysis. These considerations led us to try SPC estimation of finger movements with the

Myo armband, namely to estimate the angles between finger phalanges through a regression model for each finger joint that expressed the joint angle according to selected sEMG features, extracted from the sEMG sensor signals. Although the measurements of the angles refer to four different postures, they are used all together to build a global regression model that creates an interpolation between the individual postures.

To provide the performance evaluation of the Myo joint models in terms of repeatability, reproducibility and reliability, we referred to a standard test [28], applied simultaneously to the Myo and to the data glove developed by our research lab (www.hiteg.uniroma2.it). The results of both measurement systems are then compared with those reported in the published works, applying the same test to data gloves, even with different sensing technology.

2. Materials

Solidworks was used to design two small arms, each about the size of a phalanx, jointed with a screw to rotate relative to each other. They were first placed under the finger joint to adhere to the phalanges, without any interference from the rest of the hand, then on a goniometer to read the angle with a sensitivity of 1 degree. Two rigid and cylindrical molds with thickness of 5 mm and diameters of 63 and 53 mm, respectively, were also designed. The two artworks were imported into the Makerware 3D printing CAD, to be realized with the Makerbot Replicator 2 printer operating a polylactic acid (PLA) filament, so that to provide the flexion of intermediate angles between the open and the closed hand for the Proximal Interphalangeal (PIP) and the Metacarpophalangeal (MCP) joints shown in Fig. 1.

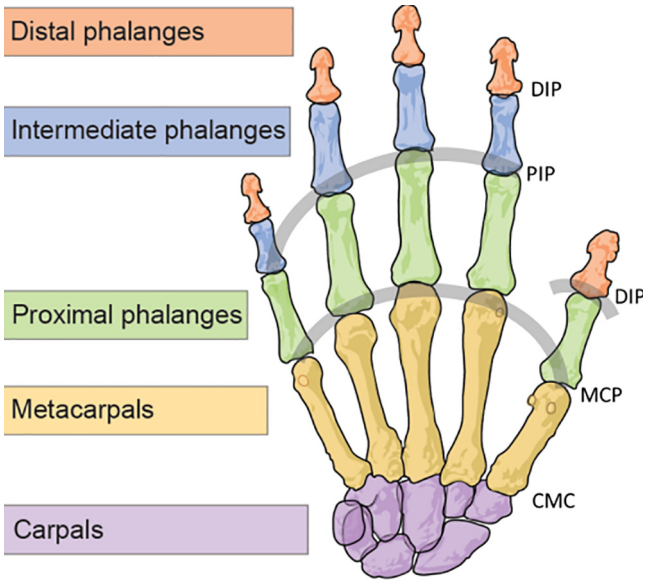

Fig. 1 – Bones and joints of the human hand. The Distal Interphalangeal (DIP) joint, the Proximal Interphalangeal (PIP) joint, the Metacarpophalangeal (MCP) joint and the Carpo-Metacarpal (CMC) joint (modified from https://en.wikipedia.org/). The 10 finger joints modeled by the glove and the Myo are highlighted with a gray trace.

2.1. *SEMG armband*

To operate sEMG, the authors used the Myo armband in this work, positioned on the proximal forearm, as indicated by Thalmic Labs, about an inch away from the biceps brachial tendon. The device embeds a 9 DoF IMU (although not used in this work) and 8 bipolar sEMG sensors with stainless steel electrodes evenly distributed on a plastic support, which is stretchable between 19 and 34 cm in circumference, to allow the electrodes to adhere to the surface of the forearm of different sizes (Fig. 2). Sensor boxes number 3, 4 and 5 are larger than the others, but the electrodes are all the same size. Its weight is only 93 g.

Fig. 3 shows the cross section of the right middle forearm (in palm supination), specifying the finger joints controlled by each muscle. All eight channels of sEMG sensors were recorded, but the strongest signals came mainly from four muscles linked to the movements of the fingers, namely A-Flexor Digitorum Profundus (electrodes n. 5–6), B-Flexor Digitorum Superficialis (electrodes n. 7–8), C-Extensor Digitorum (electrode n. 3) and D-Extensor digiti minimi (electrode n. 4). Flexion and extension movements of the thumb are controlled by the innermost muscles (dashed boxes), whose activation signals are therefore more difficult to recognize by the sEMG sensors of the Myo armband (https://teachmeanatomy.info).

As can be seen, it is virtually impossible to disambiguate the flexion of a particular finger joint from a single Myo electrode, although a correlation can be found. For example, the electrode number 4 catches EMG signal from different muscles, involved in thumb, little and wrist movements. Flexor digitorum superficialis and Flexor digitorum profundus are involved in the flexion of all fingers except the thumb, consequently the activation of the EMG signals of these muscles is a necessary but not sufficient condition to determine the flexion of a particular joint. For this reason, some works first try to classify particular gestures [23,26], where the movements

Fig. 2 – The Myo armband with the sEMG sensor numbers. The sensor number 4 should look north with palm pronation. The sensor boxes number 3, 4 and 5 are larger than the others, but the electrodes are all the same size.

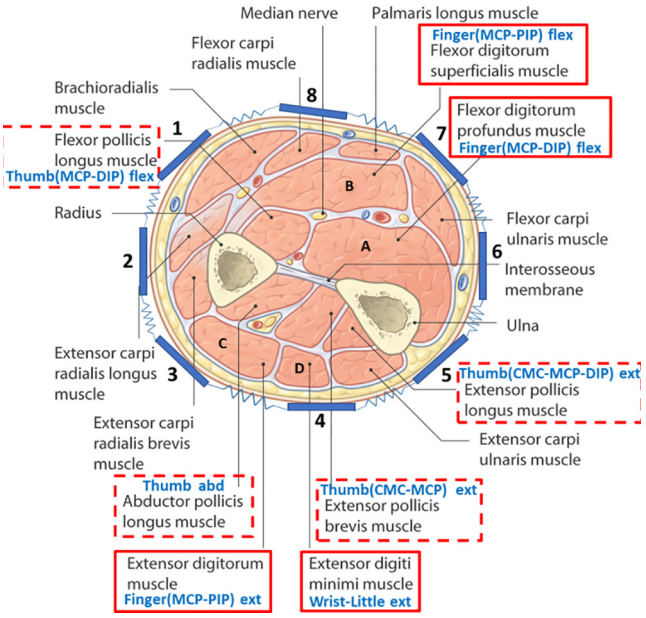

Fig. 3 – Cross section of the right middle forearm (palm supination). The octagon represents schematically the sEMG sensors of the Myo armband, with the electrode numbers. Boxed muscles are involved with flexion/extension of finger joints. Dashed boxes refer to innermost muscles.

of the fingers are more correlated, but this approach is not useful if the target is to disambiguate any original and particular hand gesture. Using an sEMG armband, the purpose of this paper is to apply the most up-to-date machine learning techniques to discover correlations between the flexion angle of each finger joint and particular patterns of sEMG signal features coming from all Myo electrodes.

The Myo armband integrates all that is needed to acquire and transfer sensor data to another unit, where they can be displayed and analyzed. sEMG signals are managed by the integrated ARM Cortex M4 Processor, which samples EMG data at 200 Hz, and transmits to a PC with a Bluetooth interface at a data rate of 115200 Hz. The open source MyoMex Matlab Software Development Kit (SDK) was used to read the sEMG data from the Bluetooth interface. The same task can be performed by a mobile device with the Myo Visualizer application, making the Myo to be very suitable to be applied in work environments.

2.2. *Data glove*

The data glove has 10 resistive flexion–extension sensors [29] of different length (1, 2, 3-inches) positioned inside sliding pockets at the proximal metacarpophalangeal (MCP) and proximal interphalangeal (PIP) joints, except for the thumb, which has an MCP sensor and a distal interphalangeal (DIP) sensor. The sensors were made by Flexpoint Sensor Systems. The glove is made of 88% polyester and 12% Elastane, because it allows greater comfort for movement. Only one medium right-hand glove was applied to the present study [7].

The Arduino Leonardo electronic board allowed the management of 10 analog inputs to read the voltage response of the bend sensors, digitally converted by a 10 bit ADC module. The sampling frequency of each sensor signal was fixed at 50 Hz. Digital data are transferred to the Bluetooth interface and transmitted to a PC with a data rate of 115200 Hz. For data transmission on 8 bit serial communication, the 10-bit data from the ADC was broken down into High and Low byte. It has a 250 g weight, largely due to the Arduino Leonardo board and the 5 V power bank. To synchronize the acquisition from the glove sensors with the tasks performed by the subjects during the test, a speaker inside the board emitted a tone, controlled by the timer of Arduino, to time the hand movements and synchronize with data acquisition.

An open source Matlab SDK was used to receive data on the PC from the Bluetooth interface. The two SDKs, respectively, for the Myo and the glove, were merged into a custom SDK to manage the data from the two different sensory units, although with different sampling rates. After recording, the two signals were aligned by numerical processing. The two sensory units were worn to perform simultaneous measurement sessions and compare their performance. The complete system is shown in Fig. 4.

3. Methods

3.1. *Test setup*

The subjects involved in the test were chosen with a very similar wrist-index distance. The glove was worn by the right hand and the electronic board was attached on the forearm between the glove and the Myo armband. The positions of the hand during the Wise test is shown in Fig. 5. The elbow was resting on a support not visible in the photo to avoid activating the antigravity muscles that can alter the sEMG signals. The measurement setup consisted of four areas: the area where to put the open hand at rest with a given reference, the big mold area, the small mold area and the closed hand area. The big mold was a cylinder of 63 mm in diameter and the small one of 53 mm. These two sizes were selected because they correspond to intermediate postures between

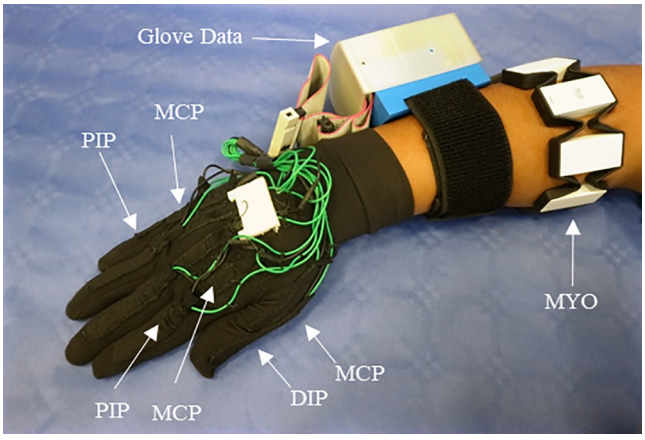

Fig. 4 – The measurement system composed of the glove, where is shown the position of the flex sensors (position on middle, ring and pinky are the same as index), the electronic board for glove data collection and transmission and the Myo armband on the forearm.

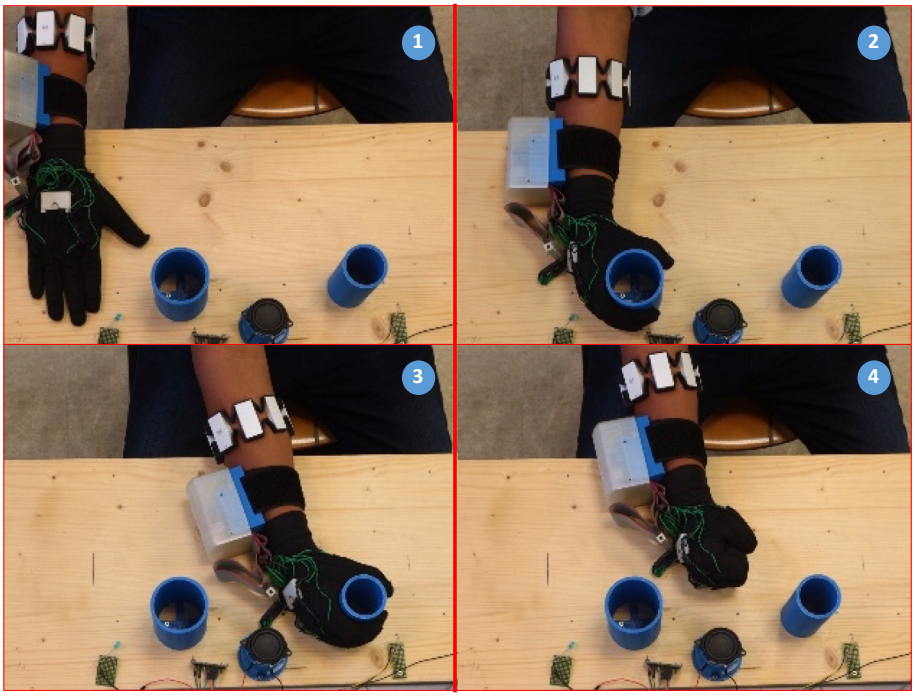

Fig. 5 – Hand postures during the Wise test (there is a speaker in the middle of the molds): 1) open hand, 2) big mold grasping, 3) small mold grasping, 4) closed hand.

the open and the closed hand: the mean values, measured with the 3D printed goniometer, were 30 degrees for MCP and PIP with the big mold, and 45 degrees for MCP and PIP with the small mold. The first mold size was chosen to compare results with those obtained in literature, the second to add an intermediate posture.

The subject was sitting on a chair with the back resting on the back of the chair, his left hand resting on his left leg and his right hand resting on the table with the palm facing down. Before starting the recording, a test was performed so that the subject acquired confidence in the test, and to check the outputs of all the sensors.

3.2. *Test protocol*

The study of the repeatability, reproducibility, reliability of similar systems was carried out by Wise [28] that introduced a test protocol to evaluate the repeatability in terms of Range (difference between highest and lowest measured angle data, in degrees) and Standard Deviation (SD) of measurements as overall errors [32]. The Wise protocol was applied in literature to data gloves of different physical principle. It consists of two different tests, test I and test II, which differ between them for the implementing rules. The test I consists of two tasks;

Task A – the subject grabs the mold on the table and kept it for a total duration of 10 s.

Task C – the subject releases the hand open on the table for the same duration.

The test II follows the same procedures of test I, where this time the task B and D correspond, respectively, to the task A and C, but, while the measuring device is never removed in test I to study the repeatability of the sensor measurements, it is removed and worn again before each block of measurements in test II to study the reproducibility of the sensor measurements.

Wise considered only two postures in his study, the open hand and the hand grasping a big mold, under the hypothesis of a linear behavior of the sensors between the two measurements [28,30,31]. As described in the setup, we extended the Wise test to evaluate two additional hand postures, namely the hand that grabs a small mold and the closed hand. Subjects were asked to apply an effort equal to about 50% of their maximum voluntary contraction (MVC) when they grabbed the molds and closed their hand.

Each trial started with the subject in the rest posture (open hand resting on the table), which was held for 10 s, then the forearm moved to grab the big mold and held it until another 10 s passed, and so on to grab the small mold and finally to close the hand. In this way, a trial is composed of four tasks: task C (open hand) – task A (big mold) – task A (small mold) – task A (closed hand). The test went on without interruptions for 10 trials of a block, during which the data acquisition did not stop. Each measurement block was repeated 10 times. To avoid muscle fatigue, a pause of at least 3 min suspended the test and the registration of data between the blocks. The measurement protocol was approved by the local ethics committee.

Some trials were carried out so that the subject became familiar with the test; the response of all sensors was controlled on the Matlab SDK. Before starting the test, the Arduino board of the glove and the Myo armband were turned on, but while Myo started the acquisition after the configuration routine, Arduino emitted an acoustic signal after 30 s, indicating the next start of the test to the subject, who had already stretched out his open hand on the table, and after 10 s another audio signal indicated the start of the test and the

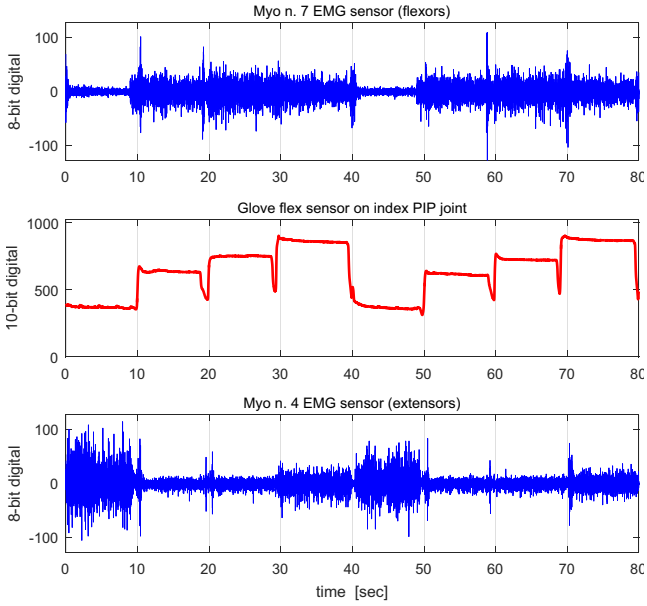

Fig. 6 – Raw digital voltage signal of two trials, each composed of 4 tasks of 10 s (open hand, big mold, small mold, closed hand), coming from number 7 (top) and number 4 (bottom) EMG sensors of the Myo armband, and the glove flex sensor on the index PIP joint (middle).

acquisition of the glove, followed by an audio signal for each change of the hand posture provided by the test protocol. Since the acquisition and transmission of the data of the two sensory units operated independently, an audio stimulus indicated the subject to close his hand with the MVC for 3 s, so that, after being recorded by the custom Matlab SDK, the two sequences were aligned by numerical processing to the signal peak, which was adopted as a time reference, after which the trials started without interruption. During the test, the SDK collected the data of each block and saved it on a file for each sensory unit. To perform the signal analysis, the two signal sequences, after aligned, were segmented in 10 s intervals, corresponding to each posture of a trial. To disregard the signal during the posture changes, and take into account any small time skew between the two sequences, only the central six seconds were considered for the analysis of each task, although the modelling results with intervals of different duration were even compared, but not presented here.

The raw digital voltage signals corresponding to the duration of two trials, each composed of four tasks, coming from the number 4 and number 7 sEMG electrodes of the Myo armband, which registered, respectively, the activation signals of the extensor muscles on the top, and of the flexor muscles on the bottom, are shown in Fig. 6, where the segment corresponding to each task includes both the movement from the previous posture and the mold grasping or the closed hand. In the central figure, the digital voltage from the flex sensor on the index PIP joint of the glove is also plotted.

4. Joint flexion models from Myo EMG

In this work, the authors tried to construct a regression model that expresses the flexion angle of 10 finger joints, corresponding to the MCP and PIP joint of each finger (MCP and DIP for the thumb), as highlighted in Fig. 1, according to the parameters extracted from the output signals of the 8 sEMG sensors. Neural networks [22] and Linear Discrimant Analysis (LDA) [23] were already applied to decode 10 DoF finger joint angles with sEMG sensors. In this work, we tried to achieve the same results with the Myo armband.

Ten right-hand volunteers, 5 males and 5 females, from 22 to 25 years with an average of 23, underwent the procedure of measuring the angle of each finger joint in each posture of the test with the printed goniometer. Subsequently, the subjects were submitted to the test I (without armband removal), composed of ten trials, but repeated only two times (2 blocks), to collect the modelling sample of sEMG sensor data in the four postures.

4.1. *Model features*

Before extraction of the signal features from the central window lasting 6 s of the 10 s signal segment of each trial, EMG signals were normalized to develop an algorithm that is not subject specific. Among the various methods proposed in literature, such as those to normalize to the MVC when the subject performed a specific isometric exercise, or to the maximum absolute value recorded by each sensor, since we noticed that the raw digital EMG signal of the Myo reached at least one time the peak value of 128 given by its 10-bit ADC, even though during the training phase the subjects were asked to perform the test with about the 50% of their MVC, we chose to normalize to the root mean square (RMS), calculated over the entire window of one block (10 trials). Different data preprocessing techniques such as rectification and digital low-pass filters [23], moving average, moving RMS [18], signal envelope were also applied to the EMG signal, but no obvious improvement in the performance of the regression models was observed.

The complexity of the responses to be obtained required the use of all the information available in an EMG signal, thus searching features related both to amplitude and time characteristics. Following a diffused approach [23,33,34], the extracted features were defined as follows:

- MAV (Mean Absolute Value) is calculated from the integral of the rectified EMG signal. It is given by:

$$MAV = \frac{1}{N}\sum_{k=1}^{N}|X_k| \tag{1}$$

where X_k is the k-sample of EMG data and N is the number of samples of the chosen window.

- RMS (Root Mean Square) is given by:

$$RMS = \sqrt{\frac{1}{N}\sum_{k=1}^{N}X_k^2} \tag{2}$$

- WAMP (Willison Amplitude) counts every variation in the amplitude of the EMG signals that exceeds a defined threshold. It is given by:

$$WAMP = \sum_{k=1}^{N-1} f(|X_{k+1} - X_k|) \tag{3}$$

$$\text{where } f(X) = \begin{cases} 1, & X > threshold \\ 0, & otherwise \end{cases} \quad (4)$$

The threshold was adjusted to obtain features that guaranteed the best modeling performance.

- WL (Waveform Length) is the cumulative variation, which may indicate the degree of variation of the EMG signals. It is given by:

$$WL = \sum_{k=1}^{N-1} |X_{k+1} - X_k| \quad (5)$$

- ZC (Zero Crossing) counts the number of times the EMG signals cross the zero line.

$$ZC = \sum_{k=1}^{N-1} [sgn(-X_k X_{k+1}) \cap (|X_k - X_{k+1}| > threshold)] \quad (6)$$

$$\text{where } sgn(x) = \begin{cases} 1, & x > 0 \\ 0, & otherwise \end{cases} \quad (7)$$

4.2. *Model training*

The Regression Learner application from Matlab 2019 Statistical toolbox was used to train a model for the angle prediction of each finger joint, according to the features extracted from all the sEMG sensor signals, with supervised machine learning techniques. The dataset matrix with 40 columns (5 parameters for each of the 8 sensors) or predictors, and 800 rows or observations (10 trials for 2 blocks for 4 postures for 10 subjects) was created as input to the model, while the column vector with 800 elements, corresponding to the measured data with the 3D printed goniometer, was assumed as the model output or known responses. The reduction of dimension (40) of the input parameter space, with well known techniques such as Principal Component Analysis (PCA) [13,35], Nonnegative Matrix Factorization (NMF) [36], or orthogonal fuzzy neighborhood discriminant analysis [13], to refer only to some, was not attempted in this case, because, to our experience, these methods make the extracted models loose generalization.

The Matlab Regression Learner allows to compare the modelling results obtained with different training algorithms, which were tested sequentially for each finger joint model: Linear Regression (Linear, Linear Interactions, Robust Linear, Gradual Linear), Regression Trees (Fine Tree, Middle Shaft, Coarse Shaft), Support Vector Machines (SVM: Linear, Quadratic, Cubic, Fine Gaussian, Gaussian Middle, Gross Gaussian), Gaussian Process Regression (GPR: Rational Quadratic, Quadratic Expansion, Matern 5/2, Exponential), Ensembles of Trees (TE: Boosted Tree, Bagged Tree). Validation was performed using the cross-validation method, selecting 4 folds (or divisions) to partition the dataset. The app partitioned data into 4 disjoint sets or folds and, for each fold, trained a model using the out-of-fold observations, but evaluated the model performance using in-fold data, then calculated the average test error over all folds. This method provided a good estimate of the predictive accuracy of the final model that was trained using the entire data set. The statistics results were expressed as root mean square error (RMSE), correlation coefficient (R^2), mean square error (MSE), and mean absolute error (MAE), which is similar to RMSE, but less sensitive to outliers. After training the model for each finger joint, the authors selected the one with the best score, namely the lowest RMSE on the validation set. For the cross-validation method, the RMSE was calculated on all observations, counting each observation when it was in a held-out fold (not used for training), so that the score estimates the performance of the trained model on new data. The models with the best score were found to be the Rational Quadratic Gaussian Process Regression (RQGPR), the Matern 5/2 Gaussian Process Regression (MGPR) and the Boosted Tree Ensemble (BTE). For each finger joint, they are listed in Table 1 with their own statistical results and training times.

5. Myo and glove models' validation test

5.1. *Test setup*

To evaluate the performance of the Myo finger models, six healthy subjects, 3 males and 3 females, all right-handed, from 22 to 25 years with an average of 23, different from those underwent to the measuring session to extract the Myo models, were involved in the Wise test, described in Section 3.2, to simultaneously measure the response data both of the Myo and the glove and to compare the obtained results even with those found in published works by applying the same test to data gloves using different sensing technologies.

5.2. *Model calibration*

The model extracted from the training samples was calibrated on each new test subject. The bending angles of the hand joints in the four postures of the test were measured, wearing the data glove, with a manual goniometer of 1 degree resolution, to calibrate the glove models and the Myo joint models. The calibration procedure was repeated before each measurement block, finding two calibration points, obtained, respectively, from the minimum and the maximum value: for the minimum value, the subject places his open hand on the table without effort, thumbs at 45 degrees from the index and in rest, for the maximum value, the subject closes his hand with an effort equal to about 50% of the MVC. The same procedure was used to grab the mold. Each posture was held for a period of 10 s. Each period was driven by Arduino, connected to a speaker, which emitted a tone for each posture change. As usual, the signal parameters were extracted from the central window of 6 s, to disregard the signal during the posture changes.

According to a consolidated practice [7,30,31], the glove calibration was performed applying a linear interpolation between measurements of the two postures within the same test, namely between posture A and C in the repeatability test, and between posture B and D in the reproducibility test; the obtained linear model was used for mapping the digital sensor output into angular values in the following validation test.

The calibration of the Myo finger joint models on each subject was obtained from a linear transformation of the regression models, expressed by Eq. (8):

Table 1 – Statistical results and training times of the trained models for each finger joint with dataset corresponding to task A-C.

Finger	Joint	Model	RMSE [deg]	R^2	MSE [deg^2]	MAE [deg]	Training time [s]
thumb	DIP	RQGPR	9.83	0.82	96.6	7.51	58
	MCP	RQGPR	7.90	0.77	62.5	5.8	44.7
index	PIP	RQGPR	12.6	0.84	159	9.5	36.2
	MCP	BTE	7.0	0.87	48.7	4.8	11.6
middle	PIP	RQGPR	11.7	0.83	138	8.9	33.7
	MCP	RQGPR	10.9	0.84	119	8.1	44.7
ring	PIP	RQGPR	11.9	0.85	1419	9.0	37.1
	MCP	BTE	13.3	0.72	178	9.6	10.0
little	PIP	RQGPR	11.2	0.83	126	8.2	55.1
	MCP	RQGPR	10.7	0.78	115	7.5	35.7

$$\phi_{cal\ mod} = c_1 \cdot \phi_{reg\ mod}\,(EMG\,features) + c_2 \tag{8}$$

where the unknown parameters c_1 and c_2 were found imposing to Eq. (8) the satisfaction of two calibration points obtained from goniometric measurements, through the system:

$$\begin{cases} \phi_{meas\_OPEN} = c_1 \cdot \phi_{\ mod\ \_OPEN} + c_2 \\ \phi_{meas\_CLOSED} = c_1 \cdot \phi_{\ mod\ \_CLOSED} + c_2 \end{cases} \tag{9}$$

where ϕ_{meas} and $\phi_{\ mod}$ are the angles obtained, respectively, from the goniometric measurements and the regression model calculated on sEMG features extracted during the two postures described above, namely the open and the closed hand.

The calibration parameters were maintained for the duration of tasks A-C, but when the sensory systems were removed and then worn again, before each block in the task B-D, the calibration was repeated again. Moreover, the predicted angles lower than those of the open hand (i.e. negative), as well as higher than those of the closed hand, were saturated on the calibration values, respectively, because the purpose of this modeling technique is the application of Myo to prosthetic devices. For future applications of the Myo armband, however, calibration must be carried out without wearing the glove, but in this case we aimed to compare the performance of the two devices in the same conditions.

5.3. *Measurement session*

After calibration, the measurement session of the Wise test started. The period was segmented in 10 s intervals corresponding to each position, known the respective work frequency of the two sensory units. To apply the required statistical analysis, the signal processing analyzed the central 6 s window of the 10 s signal segment of each posture, to extract data of the 5 features from each of the 8 sEMG sensor signals. The joint regression models, calibrated on each subject, allowed the conversion of the extracted parameters into 10 joint flexion angles. For the glove, the voltage response of each sensor across the selected window was digitally converted, the mean value calculated over the selected window, and mapped into an angle for each finger joint.

5.4. *Statistical parameters*

After the measurement session, a code organized data in a 5-dimensional Working matrix of flexion angles, indexed by the trial number (10), block number (10), joint number (10), posture number (4) and subject (6). Then, for each posture and each subject, an array $\{X_{ijk}\}, i = 1, \cdots, 10, j = 1, \cdots, 10, k = 1, \cdots, 10$ was finally obtained for the i_{th} trial, in the j_{th} block and related to the k_{th} finger joint regression model.

A second code was used to calculate the statistical parameters, i.e. the Range and standard deviation (SD) values, the intra-correlation coefficient (ICC), and the correlation between Range and SD for all subjects. The Range for each subject, posture and finger joint was defined as [32]

$$R_k = \max_j\left(\bar{X}_{jk}\right) - \min_j\left(\bar{X}_{jk}\right) \tag{10}$$

where

$$\bar{X}_{jk} = \frac{1}{10}\sum_{i=1}^{10} X_{ijk} \tag{11}$$

is the average across the trials of each block. Then the average of R_k for each posture was calculated across all joints. The standard deviation (SD) of $\bar{X}_{jk}$ data was calculated across the blocks, then the average across the joints. Both these data, Range and SD, provide the degree of repeatability in task A-C, of reproducibility in task B-D.

The reliability between measurements within the same subject was assessed by the intraclass correlation coefficient (ICC) [29,37]. ICC was calculated for each task by randomly choosing two trials out of two randomly selected blocks for each subject, first for task A-C, then for task B-D, and then the average was calculated between trials and between blocks for each subject, then across all subjects, and finally between task A-C and B-D. If ICC approaches 1, the measurements are considered as reliable. Conversely, if the ICC approaches 0, the

low correlation is mostly due to measurement errors, indicating low reliability.

6. Test results

6.1. Repeatability and reproducibility testing

The developed code provided tabular Wise-based Range and SD data for each subject, and the average Range and SD data among all participants. Only the average values are shown in the present study.

To evaluate repeatability from task A-C, as well as reproducibility from task B-D, Table 2 compares the Range and SD data resulting from measurements performed with the Myo armband with those obtained with the glove. As expected, task C and D, which correspond to measurements with the open hand, performed always the same results, in terms of Range and SD, for the regression models of the Myo, while they change applying linear interpolation between posture A-C, in one case, and B-D, in the other case, for the glove devices.

Analysis results of Table 2 are compared in Table 3 with other gloves in literature that followed the same test. The average Range and SD data obtained with the Myo armband are in the middle of the considered scale, lower than Dipietro [32] with Hall sensors, and Wise [28] with fiber optic sensors, but higher than Gentner [30] and Simone [31] with resistive flex sensors (RFS), and Li et al. [38] with the Optical linear encoder (OLE), and much higher than O'Flinn [39] and Kortier [12] with inertial sensors (IMU), which get the best results, but with a more expensive system. For the Myo and the glove, results are related to the big mold, because it was considered the most similar to the mold used in literature to evaluate the system performance. For glove based on inertial sensors, the results for the task C and D are not reported, because doffing is not possible, since the devices have not a fabric support.

The average SD across all subjects measured through the Wise test is reported in Fig. 7 for each finger joint. For the Myo armband, the highest SD was exhibited by the middle PIP, and by the little PIP for the gloves.

6.2. Reliability testing

The reliability of each joint model was calculated as the average of 20 ICC calculations for each task, then the average across all tasks. ICC ranged from 0.75 to 0.79 (mean 0.78) for the Myo armband and from 0.71 to 0.90 with an average value across joints of 0.75 for the glove, which are compared in Table 4 with the gloves evaluated by Gentner et al. [30] (ranging from 0.81 to 0.99, mean 0.93), Simone et al. [31] (ranging from 0.79 to 0.99, mean 0.95), with the Hall sensor system of Dipietro et al. [32] (ranging from 0.7 to 1.0), and with the optical linear encoder (OLE) of Li et al. [38] (ranging from 0.88 to

Table 2 – Comparison of repeatability (task A-C) and reproducibility (task B-D) between the Myo armband and the glove, expressed as Range and SD across data resulting from the Wise test, according to the mold used.

Mold	Device	Task A		Task B		Task C (open)		Task D (open)		Mean	
		Range	SD	Range	SD	Range	SD	Range	SD	Range	SD
big	Myo	4.40	1.37	5.54	1.73	5.24	1.64	7.27	2.20	5.69	1.73
	glove	6.67	2.12	6.85	2.16	3.47	1.11	4.45	1.44	5.36	1.71
small	Myo	3.70	1.12	4.30	1.32	5.24	1.64	7.27	2.20	5.13	1.57
	glove	7.98	2.52	8.16	2.58	4.06	1.27	4.87	1.59	6.27	1.99
closed	Myo	4.85	1.50	5.54	1.77	5.24	1.64	7.27	2.20	5.73	1.78
	glove	8.18	2.60	8.91	2.92	4.31	1.14	3.55	1.40	6.24	2.01

Table 3 – Repeatability (task A-C) and reproducibility (task B-D), expressed as Range and SD across data resulting from the Wise test with the big mold of the Myo armband and the glove, are compared with those obtained by some devices with different sensor technologies from literature.

Device	Sens tech	Task A (big)		Task B (big)		Task C (open)		Task D (open)		Mean	
		Range	SD	Range	SD	Range	SD	Range	SD	Range	SD
Myo	EMG	4.40	1.37	5.54	1.73	5.54	1.64	7.27	2.20	5.69	1.73
glove	RFS	6.67	2.12	6.85	2.16	3.47	1.11	4.45	1.44	5.36	1.71
Gentner	RFS	6.09	1.94	7.16	2.26	2.61	0.86	3.98	1.28	4.96	1.59
Wise	Opt	6.5	2.6	6.8	2.6	4.5	1.6	4.4	2.2	5.6	2.3
Dipietro	Hall	7.47	2.44	9.38	2.96	3.84	1.23	5.88	1.92	6.65	2.14
Simone	RFS	5.22	1.61	–	–	1	0.5	–	–	3.36	1.05
Kortier	IMU	1.8	0.6	–	–	1.1	0.4	–	–	1.5	0.5
Li	OLE	4.56	1.57	–	–	2.02	4.56	–	–	3.29	3.07
O' Flinn	IMU	7.54	2.11	–	–	2.27	1	–	–	4.9	1.56

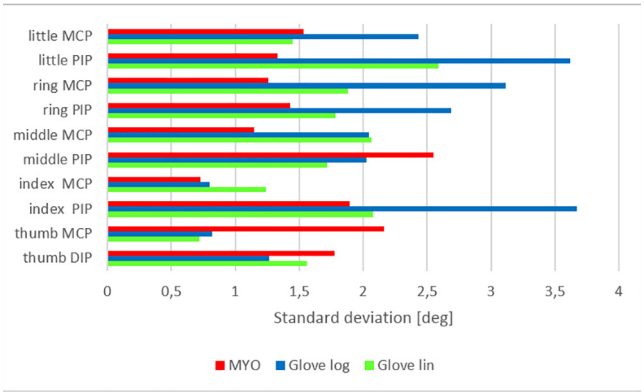

Fig. 7 – Comparison of repeatability for each finger joint between the Myo armband and the glove, measured as average SD across data from all subjects resulting from the Wise test.

Table 4 – Comparison of reliability between the Myo armband, the glove, and some devices with different sensor technology from literature, expressed as ICCs across data resulting from the Wise test.

Device	Sensing tech	ICC		
		min	max	*mean*
Myo	EMG	0.75	0.79	0.78
glove	RFS	0.71	0.90	0.75
Gentner	RFS	0.81	0.99	0.93
Dipietro	Hall	0.7	1	–
Simone	RFS	0.79	0.99	0.95
Li	OLE	0.88	0.99	0.95

0.99, mean 0.95). The average ICC for the Myo is lower than the gloves, but higher than the glove.

7. Discussion

The results obtained are hardly comparable with others, because a repeatability study with decreasing size molds does not exist in literature for the Wise test.

In Table 2 (all postures) and Table 3 (only big mold), the tasks C and D (open hand) have lower values for Range and SD than the corresponding A and B for the gloves, as declared in the previous studies [30,32], because placing the open hand on the table introduces a lower error in terms of repeatability and reproducibility than grasping a mold, which can be performed every time with not negligible variations.

One result that could not be obtained from previous studies was the variation of the Range and the SD by decrasing the size of the mold from the open hand until the hand is completely closed. The increase in the average Range was mainly due to the increase in the Range of task A and B, although with less weight in task C and D. This result is evident because, as the flexion angle of the finger joints increases, while the size of the mold towards the closed hand decreases, the linear interpolation on which the glove model is based is an increasingly less adequate approximation. An opposite result was obtained for the Myo regression models, because the muscle effort (extensors) is the highest to hold the hand open, as can be seen in Fig. 6 (bottom trace), giving higher Range and SD (5.24, 1.64), while it decreases monotonically for the closed hand (4.85, 1.50), the big mold (4.40, 1.37) and the small one (3.70, 1.12), which is the most relaxed hand posture.

The Range increased from task A to B and from C to D, as did the SD, because correlated to the Range. In fact, the doffing and donning of the measuring system before each measurement block introduces reproducibility errors both for the gloves [28,30], because the position of electrodes with respect to the joints can vary, and for the Myo, because the reference for the armband orientation is given only by a label on the top. It should be noted that Simone [31] did not provide the results for the tasks B and D. If the two tasks had been excluded from our protocol, we would have obtained an average Range of 4.97 and SD of 1.5 for the Myo.

The average (Range, SD) for males were (4.70, 1.50) lower than (6.68, 2.13) for females: the glove fit the male hand better than the female one, which did not fill the glove in the same way, while still providing a reasonable response during calibration. This was mainly due to the hand size and geometry that varied between males and females. The same difference was not observed with the Myo armband.

In Fig. 7 the glove exhibits the greatest SD for the PIP joint of the little and index fingers: the former is compressed when the hand is leaned on the table, the latter is influenced from the posture of the mold gripping [30]. The Myo models performed the highest SD for the middle PIP, because its movements are controlled by the activation signals of the same flexor/extensor muscles of other fingers, so that difficult to disambiguate, and the thumb MCP, because controlled by the activation signals of three inner muscles (Fig. 3).

The average ICC for the Myo is lower than the gloves, as we expected, because the sEMG signal amplitude and frequency are dependent by the effort, and it is rather difficult to repeat the same posture with the same effort. However, the glove achieved an even worse result with flex sensors. The ICC study was carried out for all the four postures with negligible correlation variation, indicating that the systemic error was invariant respect to the posture [30,31].

It is not easy to compare our work with more recent publications on applications of sEMG sensors to SPC of finger movements. For example, Wang presented RMSE values related to different algorithms to predict bend angles of 20 finger joints, although the models were tested on the same 5 subjects used for training [26], while we trained the models of only 10 finger joints on 10 subjects with comparable results presented in Table 1, but repeatability and reliability results are related to testing the model on 6 more subjects unused in training, which is a big challenge. About this, our model calibration technique on each subject presented in Section 5.2 can be very useful. Furthermore, as pointed out in the introduction, Wang's technique requires to classify a gesture recognition before performing the estimation of joint angles.

Chen presented an interesting work in which he attempts to decompose the gesture into single motor units with 3 grids of 64 sEMG electrodes instead of intramuscular sensors [21]; although it is undoubtedly useful to reduce the prosthetics

delay for real-time control, the presented results always refer to a single subject, so that hardly comparable with Table 1, while the generality of the model is in our opinion the most critical aspect. Furthermore, the application of these electrode arrays makes the device more difficult to use in practice than a bracelet.

Although not reported here, further investigation was devoted to understand how long should be the time interval to extract the parameters of the Myo regression models. Even if a duration of 6 s was chosen in this case, to perform the experiments in the same conditions of other studies, same results were obtained with duration as short as 2 s. This result open the way to achieve a real-time tracking of the finger movements, because, after an initial delay of 2 s, the regression parameters, as sEMG signal features, could be extracted from sliding windows of 2 s with 1 s overlapping. On the other hand, we observed that finger and thumb joint angles can be decoded accurately by the regression algorithm with latencies as short as 300 ms, calculated with a 2 GHz dual-core, 8 Gb RAM desktop computer.

8. Conclusions

To date, the measurement of finger joint angles was performed with the use of goniometric sensory gloves, even if many research studies attempted to perform the same task with EMG techniques. The novelty of our study consists mainly of two things, 1) we tested the Myo armband, a device with many advantages, such as it is very easy to use and wear without a particular care, even for a long time in a workplace, it fits different arm sizes, its results are independent from subject strength because models are trained with normalized signals, and finally it is much less expensive compared to both the gloves and discrete or integrated sEMG sensors, 2) the Myo armband, until now applied only for hand gesture classification, demonstrated for the first time to be also suitable for accurate finger posture recognition through regression models. We created models that predict the angles for each of the 10 selected MCP and PIP finger joints, without the limitations of other studies, which must first recognize the hand gesture. Limitations of our studio are that the models are obtained by interpolating static postures, which are not, however, particular gestures, but only represent the progressive closing of the hand. The repeatability and reliability of the Myo armband demonstrated to be similar to the glove developed by our lab and other data gloves using different sensing technologies and submitted to the same test, and also lied within the reliability of the manual goniometry.

Given the short time taken by the regression algorithm of the Myo armband to calculate the angles of the finger joints from sEMG parameters, this experiment paves the way to obtain real-time finger motion capture from removable and elastic myoelectric bracelet, which can be successfully applied to control prosthetic or robotic hands, because they could represent a valid alternative both to data gloves and to other sEMG devices, first of all for wearability, ease of use and cost, and in perspective also for better accuracy in the simultaneous and proportional control of finger movements.

CRediT authorship contribution statement

Antonio Pallotti: Methodology, Software, Writing - original draft. **Giancarlo Orengo:** Writing - review & editing, Visualization, Supervision. **Giovanni Saggio:** Conceptualization, Project administration.

Declaration of Competing Interest

The authors declare that they have no known competing financial interests or personal relationships that could have appeared to influence the work reported in this paper.

REFERENCES

[1] Sbernini L, Quitadamo L, Riillo F, Di Lorenzo N, Gaspari AL, Saggio G. Sensory-Glove-Based Open Surgery Skill Evaluation. IEEE Trans Hum-Mach Syst 2017;48(2):213–8.

[2] Ricci M, Terribili M, Giannini F, Errico V, Pallotti A, Galasso C, et al. Wearable-based electronics to objectively support diagnosis of motor impairments in school-aged children. J Biomech 2019;83:243–52.

[3] Ahmed MA, Zaidan BB, Zaidan AA, Salih MM, Lakulu MMB, A review on systems-based sensory gloves for sign language recognition state of the art between 2007 and 2017, Sensors, 18(7), 2018, 2208.

[4] Cavallo P, Saggio G. Conversion of sign language to spoken sentences by means of a sensory glove. J Softw 2014;9 (8):2002–9.

[5] McCaw JCS, Yuen MC, Kramer-Bottiglio R. Sensory glove for dynamic hand proprioception and tactile sensing. Proceedings of the ASME Design Engineering Technical Conference 2018;2B. https://doi.org/10.1115/DETC2018-85703.

[6] Chuang W-C, Hwang W-J, Tai T-M, Huang D-R, Jhang Y-J. Continuous finger gesture recognition based on flex sensors. Sensors 2019;19(18):3986.

[7] Saggio G, Orengo G, Pallotti A, Errico V, Ricci M, Evaluation of an integrated sensory glove at decreasing joint flexion degree. In IEEE International Symposium on Medical Measurements and Applications (MeMeA), 11-13 June 2018, Rome, Italy.

[8] Kim MK et al. Soft-packaged sensory glove system for human-like natural interaction and control of prosthetic hands. NPG Asia Mater 2019;11(1):43.

[9] Junior JCVS, Torquato MF, Noronha DH, Silva SN, Fernandes MAC. Proposal of the tactile glove device. Sensors 2019;19 (22):5029.

[10] Sorgini F, et al., Neuromorphic vibrotactile stimulation of fingertips for encoding object stiffness in telepresence sensory substitution and augmentation applications, Sensors, 18(1), 2018, 261.

[11] D'Abbraccio J, et al., Haptic glove and platform with gestural control for neuromorphic tactile sensory feedback in medical telepresence, Sensors (Switzerland), 19(3), 2019, 641.

[12] Kortier HG, Sluiter VI, Roetenberg D, Veltink PH. Assessment of hand kinematics with inertial and magnetic sensors. J NeuroEng Rehabil 2014;11:70.

[13] Al-Timemy AH, Bugmann G, Escudero J, Outram N. Classification of finger movements for the dexterous hand prosthesis control with surface electromyography. IEEE J Biomed Health Inf 2013;17(3):608–18.

[14] Shi WT, Lyu ZJ, Tang ST, Chia TL, Yang CY. A bionic hand controlled by hand gesture recognition based on surface EMG

signals: A preliminary study. Biocybern Biomed Eng 2018;38:126–35.
[15] Song W, Han Q, Lin Z, Yan N, Luo D, Liao Y, et al. Design of a flexible wearable smart sEMG recorder integrated gradient boosting decision tree based hand gesture recognition. IEEE Trans Biomed Circuits Syst 2019;13(6):1563–74.
[16] Leone F, Gentile C, Ciancio AL, Gruppioni E, Davalli A, Sacchetti R, et al. Simultaneous sEMG classification of hand/wrist gestures and forces. Front Neurorobot 2019;13:42.
[17] Velasco LES, Montiel MA, Ramírez EG, González EL. A low-cost EMG-controlled anthropomorphic robotic hand for power and precision grasp. Biohcybern Biomed Eng 2020;40:221–37.
[18] Wahid MF, Tafreshi R, Al-Sowaidi M, Langari R. Subject-independent hand gesture recognition using normalization and machine learning algorithms. J Comput Sci 2018;27:69–76.
[19] Jr Ding I, Lin RZ, Lin ZY. Service robot system with integration of wearable Myo armband for specialized hand gesture human–computer interfaces for people with disabilities with mobility problems. Comput Electr Eng 2018;69:815–27.
[20] Ngeo JG, Tamei T, Shibata T. Continuous and simultaneous estimation of finger kinematics using inputs from an EMG-to-muscle activation model. J Neuroeng Rehabil 2014;11(122).
[21] Chen Chen, Guohong Chai, WeiChao Guo, Xinjun Sheng, Dario Farina and Xiangyang Zhu, Prediction of finger kinematics from discharge timings of motor units: implications for intuitive control of myoelectric prostheses, J Neural Eng, 16(2), 2019.
[22] Hioki M, Kawasaki H, Estimation of finger joint angles from sEMG using a neural network including time delay factor and recurrent structure, Int Scholar Res Netw (ISRN) Rehabil, 2012;13, 604314.
[23] Pan L, Zhang D, Liu J, Sheng X, Zhu X. Continuous estimation of finger joint angles under different static wrist motions from surface EMG signals. Biomed Signal Process Control 2014;14:265–71.
[24] Atzori M, Gijsberts A, Castellini C, Caputo B, Hager AGM, Elsig S, et al. Electromyography data for non-invasive naturally-controlled robotic hand prostheses. Nature 2014;1:605–10.
[25] Matran-Fernandez A, Rodríguez Martínez IJ, Poli R, et al. SEEDS, simultaneous recordings of high-density EMG and finger joint angles during multiple hand movements. Sci Data 2019;6:186.
[26] Wang C, Guo W, Zhang H, Guo L, Huang C, Lin C. sEMG-based continuous estimation of grasp movements by long-short term memory network. Biomed Signal Process Control 2020;59 101774.
[27] Gijsberts A, Atzori M, Castellini C, Müller H, Caputo B. Movement error rate for evaluation of machine learning methods for sEMG-based hand movement classification. IEEE Trans Neural Syst Rehabil Eng 2014;22(4):735–44.
[28] Wise S, Gardner W, Sabelman E, Valainis E, Wong Y, Glass K, et al. Evaluation of a fiber optic glove for semi-automated goniometric measurements. J Rehabil Res Dev 1990;27 (4):411–24.
[29] Saggio G, Orengo G. Flex sensor characterization against shape and curvature changes. Sensors Actuators A Phys 2018;273:221–31.
[30] Gentner R, Classen J. Development and evaluation of a low-cost sensor glove for assessment of human finger movements in neurophysiological settings. J Neurosci Methods 2009;178:138–47.
[31] Simone LK, Sundarrajan N, Luoc X, Jia Y, Kamper DG. A low cost instrumented glove for extended monitoring and functional hand assessment. J Neurosci Methods 2007;160:335–48.
[32] Dipietro L, Sabatini AM, Dario P. Evaluation of an instrumented glove for hand-movement acquisition. J Rehabil Res Dev (JRRD) 2003;40(2):179–90.
[33] Chowdhury RH, Mamun BIR, Mohd Alauddin AB, Ashrif AAB, Kalaivani C, Chang TG. Surface electromyography signal processing and classification techniques. Sensors 2013;13:12431–66.
[34] Karabulut D, Ortes F, Arslan YZ, Adli MA. Comparative evaluation of EMG signal features for myoelectric controlled human arm prosthetics. Biocybern Biomed Eng 2017;37:326–35.
[35] Naik GR, Selvan SE, Gobbo M, Acharyya A, Nguyen HT. Principal component analysis applied to surface electromyography: A comprehensive review. IEEE Access 2016;4:4025–37.
[36] Naik GR, Nguyen HT. Nonnegative matrix factorization for the identification of EMG finger movement: evaluation using matrix analysis. IEEE J Biomed Health Inf 2015;19(2):478–85.
[37] McGraw KO, Wong SP. Forming inferences about some intraclass correlation coefficients. Psychol Methods, l 1996;1:30–46.
[38] Li K, Chen I-M, Yeo SH, Lim CK. Development of finger-motion capturing device based on optical linear encoder. J Rehabil Res Dev 2011;48(11):68–72.
[39] O'Flinn B, Sanchez JT, Tedesco S, Downes B, Connolly J, Condell J, et al. Novel smart glove technology as a biomechanical monitoring tool. Sens Transd 2015;193 (10):23–32.